JCI insight

RESEARCH ARTICLE

Intestinal epithelial potassium channels and CFTR chloride channels activated in ErbB tyrosine kinase inhibitor diarrhea

Tianying Duan,[1,2] Onur Cil,[1,3] Jay R. Thiagarajah,[4,5] and Alan S. Verkman[1]

[1]Departments of Medicine and Physiology, UCSF, San Francisco, California, USA. [2]Department of Gastroenterology, The Second Xiangya Hospital, Central South University, Changsha, Hunan, China. [3]Department of Pediatrics, UCSF, San Francisco, California, USA. [4]Division of Gastroenterology, Hepatology and Nutrition, Boston Children's Hospital, Boston, Massachusetts, USA. [5]Department of Pediatrics, Harvard Medical School, Boston, Massachusetts, USA.

Diarrhea is a major side effect of ErbB receptor tyrosine kinase inhibitors (TKIs) in cancer chemotherapy. Here, we show that the primary mechanism of ErbB TKI diarrhea is activation of basolateral membrane potassium (K^+) channels and apical membrane chloride (Cl^-) channels in intestinal epithelia and demonstrate the efficacy of channel blockers in a rat model of TKI diarrhea. Short-circuit current in colonic epithelial cells showed that the TKIs gefitinib, lapatinib, and afatinib do not affect basal secretion but amplify carbachol-stimulated secretion by 2- to 3-fold. Mechanistic studies with the second-generation TKI afatinib showed that the amplifying effect on Cl^- secretion was Ca^{2+} and cAMP independent, was blocked by CF transmembrane conductance regulator (CFTR) and K^+ channel inhibitors, and involved EGFR binding and ERK signaling. Afatinib-amplified activation of basolateral K^+ and apical Cl^- channels was demonstrated by selective membrane permeabilization, ion substitution, and channel inhibitors. Rats that were administered afatinib orally at 60 mg/kg/day developed diarrhea with increased stool water from approximately 60% to greater than 80%, which was reduced by up to 75% by the K^+ channel inhibitors clotrimazole or senicapoc or the CFTR inhibitor (R)-BPO-27. These results indicate a mechanism for TKI diarrhea involving K^+ and Cl^- channel activation and support the therapeutic efficacy of channel inhibitors.

Introduction

Diarrhea is a common side effect of cancer chemotherapy, which can be severe and dose limiting (1–4). Although many chemotherapeutic agents induce diarrhea by direct injury to the intestinal epithelium and underlying tissues with resultant mucositis, some agents may induce significant fluid secretion and would therefore be potentially amenable to therapeutics targeting intestinal ion transport mechanisms (5, 6). Small-molecule ErbB tyrosine kinase inhibitors (TKIs) are used for the treatment of a variety of cancers that overexpress ErbB receptors, including breast cancer, non-small cell lung cancer, and head and neck cancers. Previous studies have suggested that first-generation ErbB TKIs, such as gefitinib, which targets the human EGFR 1 (HER-1), and lapatinib, which targets HER-1 and HER-2, and second-generation pan–ErbB TKIs, such as afatinib, which target HER-1–HER-4, may cause diarrhea by alteration of intestinal fluid transport (7, 8). Diarrhea associated with first-generation ErbB TKIs occurs in approximately 40% to 60% of patients, with severe (grades 3–4) diarrhea in 10% to 20% of patients (9–11). Diarrhea is even more of a problem with second-generation inhibitors, such as afatinib, with greater than 90% of patients affected and a greater incidence of severe diarrhea (9, 12). Current management of ErbB TKI–associated diarrhea includes fluid replacement, antimotility agents such as loperamide, and in severe cases, TKI dose reduction or discontinuation (13). Given the morbidity and reduced clinical effectiveness associated with severe diarrhea following ErbB TKI therapy, there remains an unmet need for efficacious, targeted, and safe antidiarrheal therapies.

Intestinal fluid secretion results from active chloride (Cl^-) secretion by intestinal epithelial cells (enterocytes) into the intestinal lumen. This involves Cl^- entry into cells from the basolateral or blood side via the Na^+-K^+-$2Cl^-$ (NKCC1) cotransporter and exit into the intestinal lumen though cAMP and Ca^{2+}-activated Cl^- channels (CaCCs) (14–16). The driving force for Cl^- secretion is created by the Na^+/K^+ pump on the cell basolateral membrane acting in concert with basolateral membrane K^+ channels, which establishes an

Conflict of interest: ASV is a named coinventor on a CFTR inhibitor patent application (9062073), whose rights are owned by the University of California.

Submitted: November 26, 2018
Accepted: January 14, 2019
Published: January 22, 2019

Reference information:
JCI Insight. 2019;4(4):e126444.
https://doi.org/10.1172/jci.insight.126444.

interior-negative cell potential that creates the electrochemical gradient driving Cl^- efflux across the apical membrane (16, 17). Several toxin-mediated infectious diarrheas, such as cholera and *Rotavirus* diarrhea, involve increased epithelial intracellular second messengers, such as cAMP and Ca^{2+}, resulting in activation of CF transmembrane conductance regulator (CFTR) or CaCCs at the apical membrane of enterocytes and K^+ channels at the basolateral membrane. We previously demonstrated the efficacy of Cl^- channel inhibitors in experimental animal models of enterotoxin-mediated secretory diarrheas (18–20). Although previous studies have shown that EGF signaling can alter epithelial Cl^- transport (21, 22), the mechanisms involved in ErbB TKI–induced diarrhea as well as the potential efficacy of ion channel–targeted drug candidates remain unknown.

We therefore sought to investigate the effect of ErbB TKIs on epithelial ion and fluid transport and the potential therapeutic efficacy of ion channel–targeted drug candidates. We discovered that ErbB TKIs induce diarrhea by a unique secretory mechanism involving activation of basolateral K^+ channels and apical CFTR Cl^- channels. Using an experimental rat model of afatinib-induced diarrhea, we demonstrate the efficacy of K^+ and Cl^- channel inhibitors in reducing diarrhea, including the FDA-approved drug clotrimazole, the investigational drug senicapoc, and the preclinical CFTR inhibitor benzopyrimido-pyrrolo-oxazine-dione 27 (BPO-27).

Results

ErbB TKIs amplify carbachol-induced current in intestinal cells. Because previous reports have implicated EGFR signaling in intestinal Cl^- and fluid secretion (21, 22), we initially tested the effect of 2 first-generation ErbB TKIs, lapatinib and gefitinib, and a second-generation pan-ErB TKI, afatinib, on Cl^- secretory responses in T84 human colonic epithelial cells. Short-circuit current was measured in T84 cell monolayers with identical solutions bathing the apical and basolateral surfaces. Figure 1A shows that administration of ErbB TKIs alone does not increase short-circuit current, suggesting that they do not directly activate apical membrane Cl^- channels, such as CFTR or CaCCs, or other transporters involved in generating a secretory current, such as basolateral K^+ channels. However, addition of the ErbB TKIs before the muscarinic agonist carbachol greatly amplified the subsequent Cl^- secretory response by 2- to 3-fold. ErbB TKIs also amplified Cl^- secretion induced by the purinergic agonist ATP and the Ca^{2+} ATPase inhibitor thapsigargin (Supplemental Figure 1; supplemental material available online with this article; https://doi.org/10.1172/jci.insight.126444DS1), indicating that the TKI effect is not specific for cholinergic agonists. Given that patients receiving second-generation pan–ErbB TKIs have the highest incidence of diarrhea (9, 12, 13), subsequent mechanistic and therapeutic studies were done with afatinib.

Figure 1B shows that, as in T84 cells, afatinib did not by itself increase short-circuit current in mouse ileum but amplified the current response to carbachol.

To test whether the effect of afatinib involves EGF signaling, short-circuit current was measured in cells pretreated with EGF alone, afatinib alone, or EGF together with afatinib (Figure 1C). Administration of EGF greatly reduced Cl^- secretion in response to carbachol. Afatinib overcame the EGF-mediated suppression of carbachol-induced current, with similar current responses seen for cells pretreated with afatinib alone versus EGF plus afatinib. The blocking of the EGF suppression of carbachol-induced current by afatinib suggests that its amplification of the Cl^- secretory response occurs via its primary mechanism of action — inhibition of ErbB receptor activation.

We next determined the time course and concentration dependence of the afatinib-induced amplification of the carbachol response in T84 cells. Figure 2A shows the amplifying effect of afatinib on carbachol-induced short-circuit current increased with time between afatinib and carbachol additions, with half maximal effect at 10 to 15 minutes and maximal effect seen by approximately 25 minutes. When added 25 minutes before carbachol, the afatinib effect was concentration dependent, with EC_{50} approximately 5 μM (Figure 2B).

Afatinib-mediated amplification of carbachol-induced Cl^- secretion is CFTR dependent. Because carbachol induces Cl^- secretion through activation of intracellular Ca^{2+} signaling and activation of the apical membrane CaCC, we investigated whether the afatinib-induced amplification of the carbachol response involves Ca^{2+} elevation and CaCC activation. Figure 3A shows that the CFTR-selective inhibitor BPO-27 had little effect on the carbachol-induced current in T84 cells. However, BPO-27 blocked the afatinib augmentation of the carbachol-induced current. Treatment with BAPTA-AM to block elevation of intracellular Ca^{2+} largely prevented the carbachol response. However, in the BAPTA-treated cells afatinib produced a substantial residual carbachol response, which was blocked by the 2 chemically unrelated CFTR inhibitors BPO-27

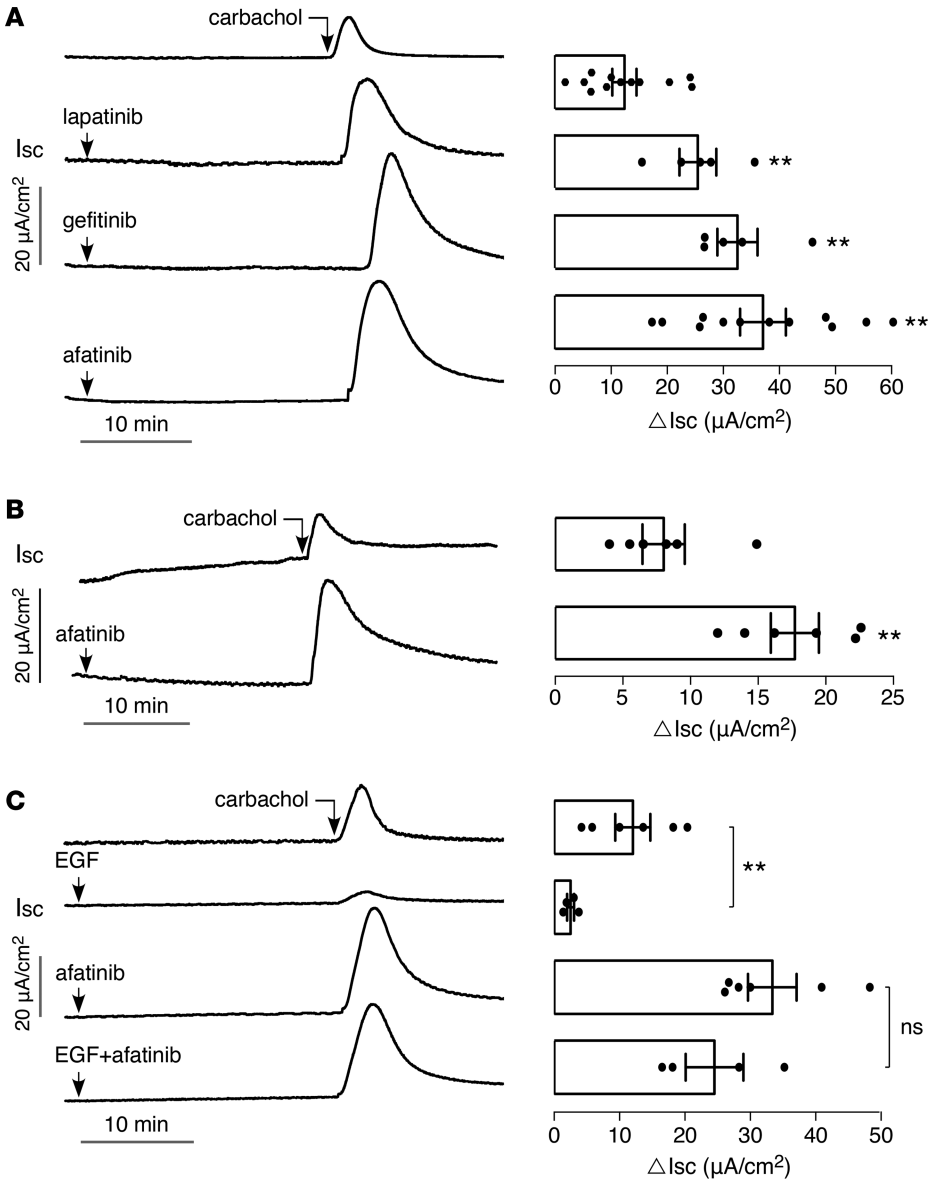

Figure 1. TKIs amplify carbachol-induced current in T84 cells. (**A**) (Left) short-circuit current (I_{sc}) in T84 cells showing responses to 40 μM lapatinib, 20 μM gefitinib, and 20 μM afatinib, added 25 minutes before 100 μM carbachol. (Right) summary of peak carbachol-induced current (ΔI_{sc}, mean ± SEM, n = 5–12). (**B**) (Left) short-circuit current in mouse ileum showing responses to 20 μM afatinib added 25 minutes before 200 μM carbachol. (Right) summary of peak current (mean ± SEM, n = 6). (**C**) (Left) short-circuit current in T84 cells showing responses to 100 ng/ml EGF and 20 μM afatinib, alone and together, added 25 minutes before 100 μM carbachol. (Right) summary of peak current (mean ± SEM, n = 4–6). $^{**}P < 0.01$, by 2-tailed t test.

and $CFTR_{inh}$-172. Of note, the carbachol response curves were broader (slower return to baseline) in the presence than the absence of afatinib.

Figure 3A summarizes the carbachol response as the maximum increase in short-circuit current (ΔI_{sc}). The data suggest that afatinib augmentation of the carbachol-induced Cl^- secretion is CFTR dependent and does not require Ca^{2+} signaling. The amplified current was blocked by CFTR inhibitors, was not prevented by BAPTA treatment, and had a different character than the Ca^{2+}-dependent carbachol response in terms of its curve shape as quantified by $t_{1/2}$ analysis (Figure 3B).

Afatinib does not affect calcium or cAMP signaling. The residual afatinib-amplified carbachol current in BAPTA-treated cells and its suppression by CFTR inhibitors suggested that the afatinib effect is not mediated by intracellular Ca^{2+} signaling but perhaps could involve cAMP signaling. Consistent with this, afatinib did not by itself increase cytoplasmic Ca^{2+} concentration (data not shown), nor did it have a significant effect on the transient elevations in Ca^{2+} concentration following ATP or carbachol (Figure 4A). Also, afatinib did not itself increase total cellular cAMP, nor did it affect the increase in cAMP following forskolin (Figure 4B).

Afatinib amplifies carbachol-induced activation of basolateral K^+ channels and apical CFTR Cl^- channels. Though afatinib did not affect cAMP levels, the possibility was investigated that afatinib might influence forskolin-induced (cAMP-induced) short-circuit current. Interestingly, as found with carbachol, afatinib

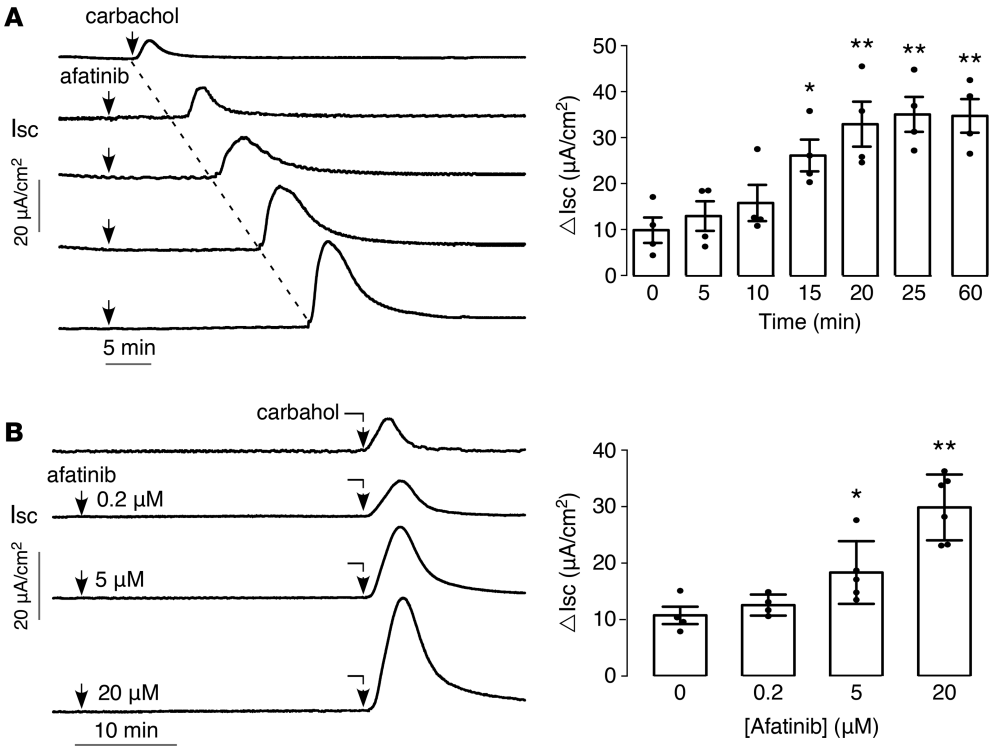

Figure 2. Time course of action and concentration dependence of afatinib's amplification of carbachol response. (**A**) (Left) time course of afatinib effect on carbachol-induced short-circuit current in T84 cells. Cells treated with 20 μM afatinib for different times before 100 μM carbachol. (Right) summary of peak carbachol-induced current (mean ± SEM, $n = 4$). (**B**) (Left) concentration dependence of afatinib effect. (Right) summary of peak current (mean ± SEM, $n = 4–6$). $^*P < 0.05$, $^{**}P < 0.01$, by 2-tailed t test.

amplified the forskolin-induced current response (Figure 5A), albeit to a lesser extent than seen with carbachol. This result, with the lack of effect of afatinib on intracellular Ca^{2+} and cAMP and the finding that afatinib itself does not induce a current response, suggests that the afatinib amplification of the Cl^- secretory response may in part involve activation of basolateral membrane K^+ channel(s). In support of this possibility, the afatinib response was mimicked by 1-Ethyl-1,3-dihydro-2H-benzimidazol-2-one (EBIO), a K^+ channel agonist that increases the conductance of both the epithelial Ca^{2+}- and cAMP-activated K^+ channels (23), though one study reported that EBIO might at higher concentrations activate an apical chloride conductance in T84 cells (24). Figure 5B shows that EBIO pretreatment amplifies the carbachol and forskolin current responses. Pretreatment with EBIO and afatinib together showed a similar effect to pretreatment with EBIO alone.

The FDA-approved antifungal drug clotrimazole is a well-characterized inhibitor of the intermediate-conductance Ca^{2+}-activated K^+ channel (KCa3.1) and the epithelial cAMP-activated K^+ channel (25), and the chemically related investigational drug senicapoc is an inhibitor of KCa3.1 (26). In T84 cells, clotrimazole or senicapoc largely prevented the carbachol- and forskolin-induced current responses, both without and with afatinib pretreatment (Figure 6). The small residual current probably is because of the presence of other K^+ channels(s) rather than incomplete inhibition by clotrimazole or senicapoc, because higher concentrations of these compounds did not inhibit the residual current (data not shown); in patch-clamp studies clotrimazole has been reported to fully inhibit epithelial Ca^{2+}-activated K^+ channels (27). Supplemental Figure 2 shows low micromolar IC_{50} for inhibition of Ca^{2+}- and cAMP-dependent basolateral K^+ conductances by clotrimazole and senicapoc.

To measure basolateral membrane K^+ conductance directly, short-circuit current was measured in T84 cells following permeabilization of the apical membrane with amphotericin B in Cl^-- and Na^+-free solutions and an apical-to-basolateral K^+ gradient (Figure 7A). Afatinib pretreatment produced an increase by approximately 2-fold in the carbachol response, which was largely blocked by clotrimazole. Afatinib therefore amplifies the opening of basolateral membrane K^+ channel(s) in response to carbachol in T84 cells.

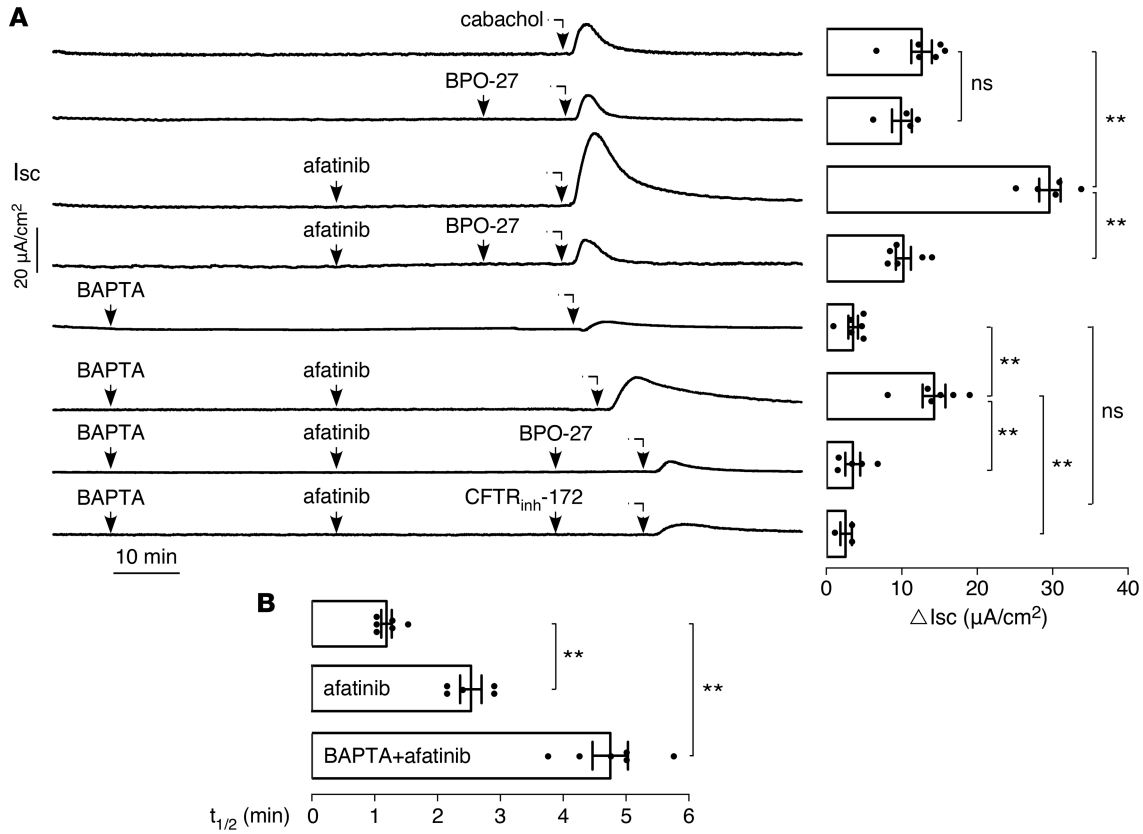

Figure 3. The afatinib-induced augmentation in carbachol current is CFTR dependent. (**A**) (Left) short-circuit current in T84 cells showing effects of 20 μM afatinib, 100 μM carbachol, 10 μM BPO-27, and 10 μM $CFTR_{inh}$-172, with or without 30 μM BAPTA-AM, as indicated. (Right) summary of peak carbachol-induced current (mean ± SEM, n = 3–6). (**B**) Half-time ($t_{1/2}$) of the decreasing phase of the carbachol response curve (mean ± SEM, n = 5–6). $^{**}P <$ 0.01, by 2-tailed t test.

In addition to afatinib's action on amplifying basolateral K^+ channel activation, the data in Figure 2 suggest that afatinib also amplifies apical CFTR Cl^- channel activation. To test this, short-circuit current was measured following permeabilization of the basolateral membrane and with a basolateral-to-apical Cl^- gradient (Figure 7B). Afatinib pretreatment produced a greater than 4-fold increase in the carbachol response, which was blocked by BPO-27. The amplified carbachol response with afatinib therefore also involves increased activation of apical membrane CFTR Cl^- channels.

Signaling pathways involved in afatinib modulation of K^+ and Cl^- channels. Figure 8A shows a proposed mechanism for afatinib action as deduced from the data above and prior published work on EGF signaling in intestinal epithelia (28, 29). EGF/TKI modulation of basolateral K^+ and apical Cl^- activation is shown, with Ca^{2+}-independent signaling involving ERK and PKC pathways. We used selective ERK and PKC inhibitors to investigate their involvement in afatinib signaling. Supplemental Figure 3 shows that the PKC and ERK inhibitors largely overcome the inhibitory effect of EGF on the carbachol-induced short-circuit current in T84 cells, both in the absence and in the presence of BAPTA suppression of Ca^{2+}-signaling, and that the amplified current is inhibited by BPO-27. Figure 8B shows that ERK and PKC inhibition largely recapitulate the afatinib effect on carbachol-induced short-circuit current and that the combined effect of afatinib with PKC and ERK inhibition is similar to that of afatinib alone. These results support involvement of PKC and ERK signaling in the afatinib effect on modulation of ion channel activity.

Afatinib-induced diarrhea in rats is reduced by inhibitors of K^+ channels and CFTR Cl^- channels. Following initial dose-finding studies in mice and rats with several TKIs, using stool water content (from wet and dry weight measurement) as the endpoint, a robust, short-term experimental animal model of afatinib diarrhea was established involving daily oral administration of 60 mg/kg afatinib in rats. By days 4 to 5, stool water content, determined by stool wet/dry weight ratio, increased to greater than 80% compared with the baseline of approximately 60% (Figure 9A). Examination of intestinal histology showed only minor-to-moderate pathology up to day 4 but greater epithelial disruption after that

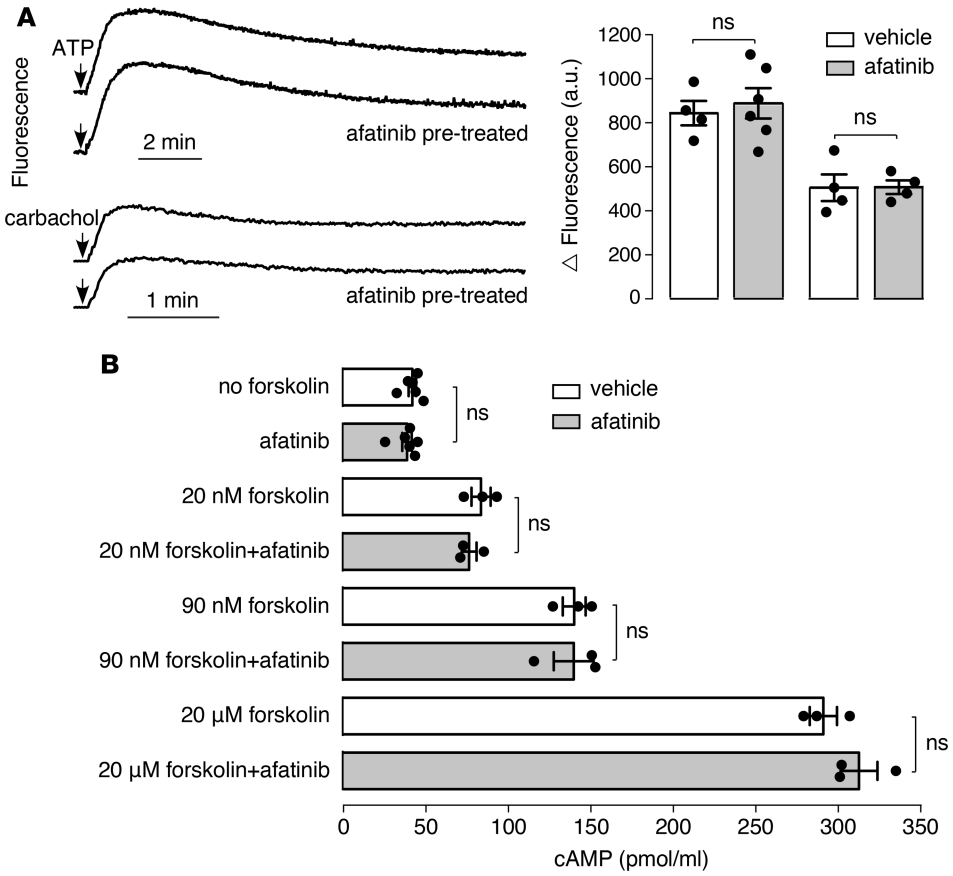

Figure 4. Afatinib does not affect calcium or cAMP signaling. (**A**) (Left) cytoplasmic Ca^{2+} concentration measured by Fluo-4 fluorescence. Afatinib (20 μM) was added 20 minutes before addition of 100 μM ATP or 100 μM carbachol. (Right) peak increase in Fluo-4 fluorescence after ATP or carbachol (mean ± SEM, *n* = 4–6). (**B**) cAMP in T84 cells measured 30 minutes after incubation with afatinib (20 μM) or forskolin (20 nM, 90 nM, 20 μM), with or without afatinib (20 μM) (mean ± SEM, *n* = 3–6). Not significant, by 2-tailed *t* test.

(Supplemental Figure 4). A 5-day afatinib model was then used to test the potential antidiarrheal effect of the K^+ channel blockers clotrimazole and senicapoc and the CFTR inhibitor BPO-27. In principle, inhibition of either basolateral or apical rate-limiting ion channels could be effective in reducing intestinal fluid secretion, particularly in view of their activation by afatinib.

Treatment of rats with BPO-27 at 10 mg/kg intraperitoneally twice daily, starting 1 day after the first afatinib dose, produced a significant reduction in the increased stool water content with afatinib (Figure 9B). The BPO-27 dosing was selected from prior pharmacokinetics data in mice (18) and preliminary studies in rats (data not shown) to produce predicted therapeutic concentrations in serum. The increase in stool water content was inhibited by approximately 50% on days 3 and 4. The reduced inhibitor effect by day 5 may be related to afatinib-induced mucosal injury in this model and hence a secondary injury–related diarrheal mechanism that is relatively insensitive to ion channel blockers.

Oral treatment of rats with clotrimazole at 100 mg/kg (oral in 2 divided doses), a dose and administration regimen chosen from published data (30–32), also significantly reduced the increase in stool water content in afatinib-treated rats, with approximately 75% inhibition on days 3 and 4 (Figure 9C). Significant, though lesser, reduction in the increase in stool water content was found for senicapoc at 30 mg/kg twice daily, a dose chosen from published data (Figure 9D) (33, 34). These various maneuvers had little effect on body weight (Supplemental Figure 5). Given the substantial antidiarrheal effects of BPO-27 and clotrimazole, we tested both compounds together (Figure 9E), speculating that full suppression of increased stool water might occur. However, the combined effect of BPO-27 and clotrimazole was not greater than the effect of each compound used individually, which may reflect a maximum effect on ion channel blockers or intestinal mucosal injury when both compounds are used together.

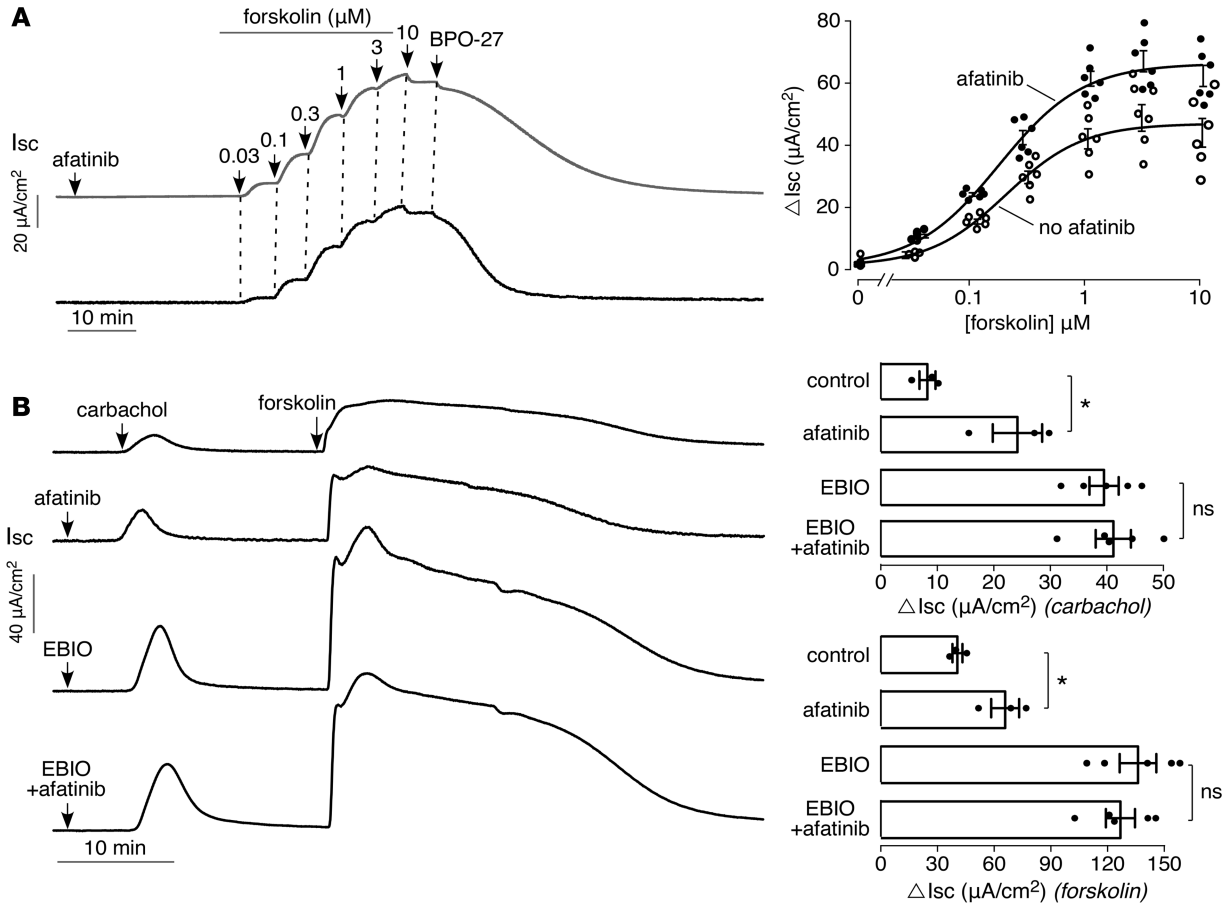

Figure 5. Afatinib amplifies forskolin-induced current in T84 cells. (**A**) (Left) short-circuit current in T84 cells in response to 20 μM afatinib (or vehicle control) followed by indicated concentrations of forskolin, then 10 μM BPO-27. (Right) forskolin concentration dependence of short-circuit current (mean ± SEM, *n* = 6). (**B**) (Left) short-circuit current in T84 cells in response to additions of EBIO (500 μM) and/or afatinib (20 μM) added 25 minutes before 100 μM carbachol followed by 10 μM forksolin. (Right) summary of peak carbachol- and forskolin-induced currents (mean ± SEM, *n* = 3–5). **P* < 0.05, by 2-tailed *t* test.

Discussion

The study here establishes a unique cellular mechanism for secretory diarrhea and suggests a pharmacological approach to treat TKI-induced diarrhea. Secretory diarrheas produced by bacterial enterotoxins, such as cholera toxin of *Vibrio cholerae* in cholera and heat-stable enterotoxin of *Escherichia coli* in traveler's diarrhea, activate apical membrane CFTR Cl^- channels by elevation of cyclic nucleotide levels in enterocytes (14, 35, 36). Additional mechanisms in these diarrheas include activation of cAMP-dependent K^+ channels at the basolateral membrane and reduced activity of proabsorptive ion transporters, such as sodium/hydrogen exchanger 3 (37, 38). Viral enterotoxins, such as nonstructural protein 4 in *Rotavirus* diarrhea, cause intestinal fluid secretion in part by elevation of cytoplasmic Ca^{2+} and consequent activation of apical CaCCs and basolateral Ca^{2+}-dependent K^+ channels (39). The mechanism of TKI diarrhea established here — amplified activation of basolateral K^+ channels and apical CFTR Cl^- channels — is distinct from known secretory diarrhea mechanisms. This unique mechanism may occur in other diarrheas as well.

Several observations support the conclusion that ErbB TKI–induced diarrhea involves amplification of basolateral K^+ and apical CFTR Cl^- channel function in intestinal epithelial cells, as diagrammed in Figure 8A. Though afatinib did not by itself increase short-circuit current in T84 cells, it amplified short-circuit current responses to carbachol or forskolin, and the afatinib-dependent component of the amplified current was blocked by CFTR inhibitors. Direct evidence for amplification of basolateral K^+ channel and apical CFTR Cl^- channel activation was found in Figure 7 using selective membrane permeabilizations with amphotericin B, with ion substitution and ion gradients. Mechanistically, increased basolateral membrane K^+ conductance facilitates transcellular Cl^- secretion by membrane hyperpolarization and an increased electrochemical driving force for Cl^- exit through open apical Cl^- channels. Afatinib's action in amplifying basolateral K^+ conductance

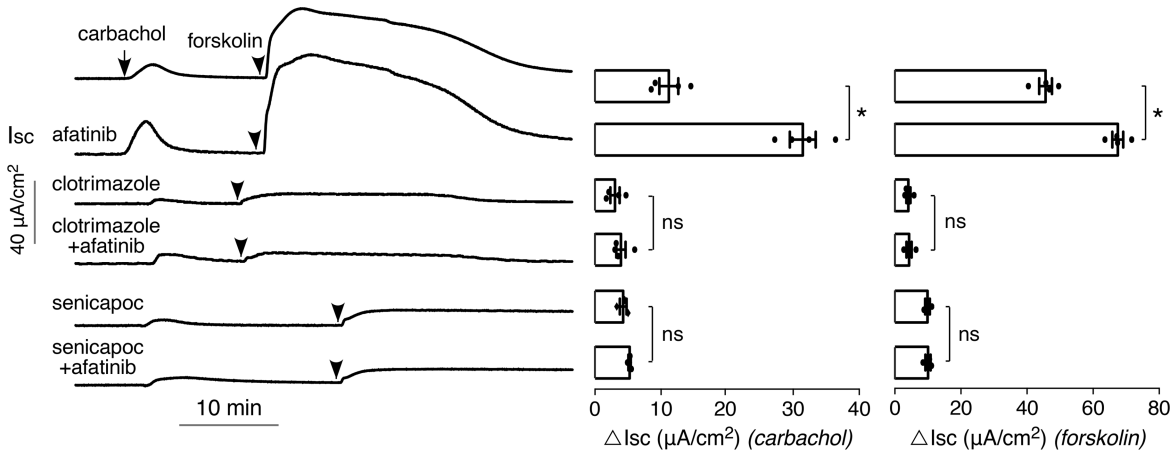

Figure 6. K⁺ channel inhibitors block the afatinib-induced augmentation in carbachol current. (Left) short-circuit current in T84 cells treated with 20 μM afatinib, 30 μM clotrimazole, and/or 10 μM senicapoc, as indicated, 30 minutes before addition of 100 μM carbachol followed by 10 μM forskolin. (Right) summary of peak carbachol- and foskolin-induced peak current (mean ± SEM, n = 3–4; $^*P < 0.05$, by 2-tailed t test).

together with apical CFTR Cl^- conductance is predicted to be particularly effective in promoting intestinal secretion. These findings suggest the potential therapeutic efficacy of blocking basolateral membrane K^+ channels or apical membrane CFTR in diarrhea caused by ErbB TKIs.

In an experimental rat model of afatinib diarrhea, the K^+ channel inhibitors clotrimazole and senicapoc, and the CFTR inhibitor BPO-27, each produced a clear-cut reduction in the increase in stool water content following afatinib. Clotrimazole and senicapoc are structurally similar triphenylmethanes with IC_{50} of 11 nM and 100 nM, respectively, for inhibition of the human Gardos channel (26, 40). Clotrimazole is a commonly used topical antifungal drug for cutaneous, oral, and vaginal fungal infections (41). Clotrimazole inhibits Cl^- secretion in T84 cells stimulated by cAMP, cGMP, and Ca^{2+} agonists and is thus considered a general inhibitor of intestinal basolateral K^+ channels, with an IC_{50} of approximately 500 nM, much higher than its IC_{50} for the Gardos channel (25). However, oral clotrimazole is no longer used because of its very short elimination half-life and significant side effects, including hepatotoxicity (42–44). The chemical analog senicapoc is an investigational drug that has been tested in clinical trials for sickle cell disease and shown to have very long elimination half-life (~2 weeks) in humans and to be well tolerated (45, 46). We found that senicapoc also inhibits basolateral K^+ conductance in T84 cells with comparable potency to clotrimazole. (R)-BPO-27 is a selective CFTR inhibitor with low nanomolar potency that has shown efficacy in experimental mouse models of cholera and traveler's diarrhea (18), as well as in autosomal polycystic kidney disease in which fluid accumulation in kidney cysts is CFTR dependent (47).

Our study supports a mechanism of afatinib diarrhea involving potentiation of apical CFTR Cl^- channels and basolateral K^+ channels. We note recent reports concluding that the TKI dacomitinib activates apical Cl^- channels without specifying which channels and without investigation of basolateral K^+ channels (48). They also reported that the antidiarrheal drug crofelemer, which acts in part by inhibition of apical CaCCs (49), increased rather than reduced dacomitinib diarrhea in rats. Our results would predict no beneficial effect of crofelemer in TKI diarrhea, and in preliminary studies (not shown) we found no beneficial effect of crofelemer in the afatinib diarrhea model used herein. Results are awaited of clinical trials of crofelemer in TKI diarrhea (NCT02910219 and NCT03094052).

Cl^- secretion by enterocytes involves Cl^- entry into the basolateral membrane, which is mediated primarily by NKCC1 and AE2 and requires a functional Na^+/K^+-ATPase and basolateral K^+ conductance. Basolateral K^+ conductance can be rate limiting for Cl^- exit across the apical membrane through CFTR and CaCCs (50). Basolateral K^+ channels are regulated by distinct signaling mechanisms including cAMP and Ca^{2+}. Several K^+ channels are expressed in the basolateral membrane of intestinal crypt cells, including KCNE3, KNCQ1, KCNK5, KCNN4 (Gardos channel), and KCNJx (51, 52). Here, we found that afatinib augments the activity of K^+ channels activated by cAMP and Ca^{2+} agonists, which clotrimazole and senicapoc inhibited. Though clotrimazole and senicapoc have relatively low potency for inhibition of intestinal epithelial K^+ channels, drug discovery efforts may identify more potent inhibitors for treating of ErbB TKI diarrhea. Identification of the K^+ channels afatinib activates in different segments of human intestine may be helpful as well.

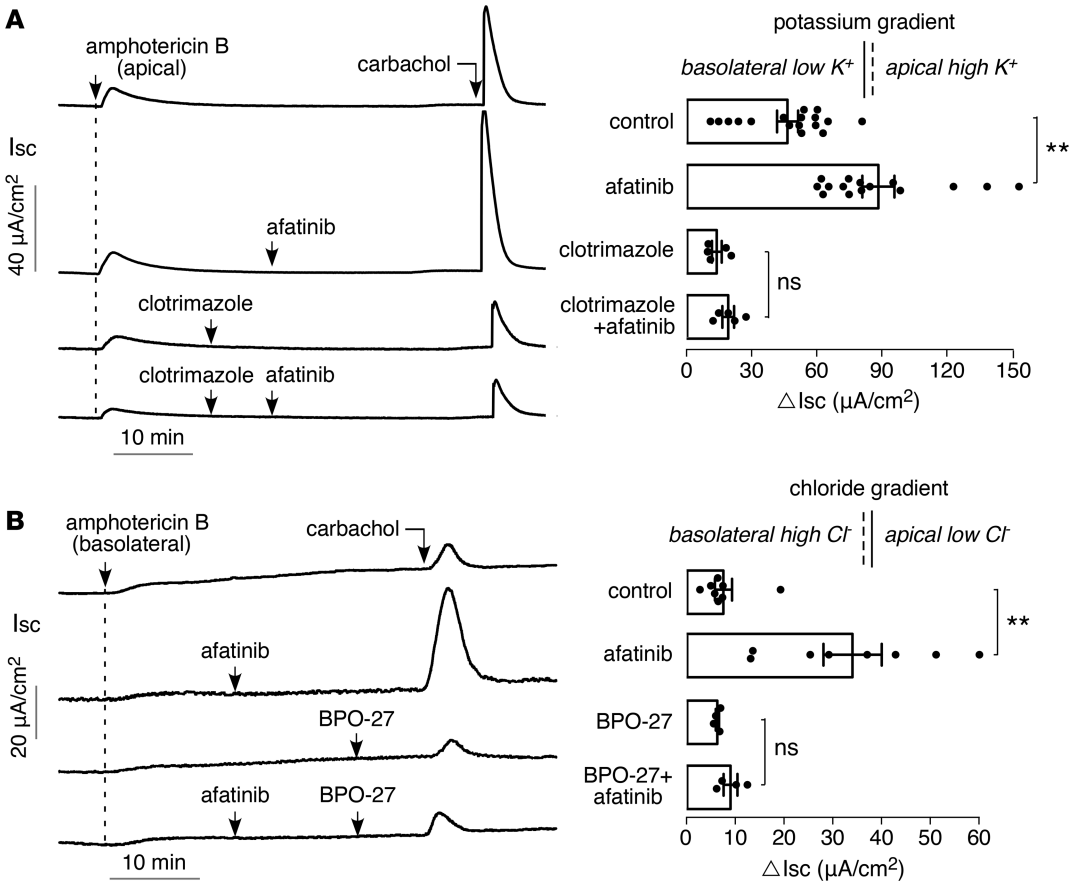

Figure 7. Afatinib amplifies carbachol-induced activation of basolateral K^+ conductance and apical CFTR Cl^- conductance. (**A**) (Left) short-circuit current in T84 cells following apical membrane permeabilization with 20 μM amphotericin B in the presence of an apical-to-basolateral solution K^+ gradient (apical [K^+] 142 mM, basolateral [K^+] 5 mM). Afatinib (20 μM) and carbachol (100 μM) added as indicated. (Right) summary of peak carbachol-induced current (mean ± SEM, n = 5–17). (**B**) (Left) short-circuit current in T84 cells following basolateral membrane permeabilization with 250 μg/ml amphotericin B in the presence of a basolateral-to-apical solution Cl^- gradient (basolateral [Cl^-] 120 mM, apical [Cl^-] 5 mM). Afatinib (20 μM), BPO-27 (10 μM), and carbachol (100 μM) were added as indicated. (Right) summary of peak carbachol-induced current (mean ± SEM, n = 4–8). $^{**}P < 0.01$, by 2-tailed t test.

Our studies suggest that the mechanism by which afatinib increases Cl^- secretion in intestinal epithelial cells involves release of inhibitory pathways that modulate basolateral membrane K^+ conductance and apical membrane CFTR Cl^- conductance. Although the detailed signaling mechanisms by which this occurs remain to be established, our data with previous data by Barrett and coworkers (22, 28, 53, 54) suggest that Ca^{2+}-independent ERK and PKC signaling modulate intestinal epithelial K^+ and Cl^- conductances. Previous studies have shown that activation of muscarinic receptors not only elevates cytoplasmic Ca^{2+} (through phospholipase C and 1,4,5-inositol trisphosphate release) but also causes EGFR transactivation resulting in ERK signaling (55, 56). Muscarinic receptor activation also activates PKC, which in epithelial cells can lead to ERK pathway activation (57). ERK activation and subsequent kinase activity have been shown to downregulate epithelial K^+ and Cl^- channel activity and inhibit secretion (54, 58, 59), in agreement with our data showing that ERK and PKC inhibition can recapitulate ErbB TKI–mediated amplification of short-circuit current. Therefore, the data here suggest that ErbB TKIs induce Cl^- secretion by preventing EGF-mediated ERK activity, which normally acts to limit both basolateral K^+ and apical Cl^- channel activity. Loss of ERK-mediated inhibition therefore results in amplified channel activity and excessive fluid secretion. Further studies are needed to elucidate the details of how ERK signaling alters K^+ and Cl^- channel function and the precise roles of PKC and cAMP pathways in ERK-mediated alterations in channel function.

In conclusion, the data here support a prosecretory mechanism for ErbB TKI diarrhea involving amplified activity of K^+ channels at the basolateral membrane of intestinal epithelial cells and CFTR Cl^- channels at the apical membrane. Notwithstanding the limitations of the approved and investigational K^+ channel blockers, our data support their testing in human TKI diarrhea, as well as testing of CFTR inhibitors once they are advanced to clinical trials.

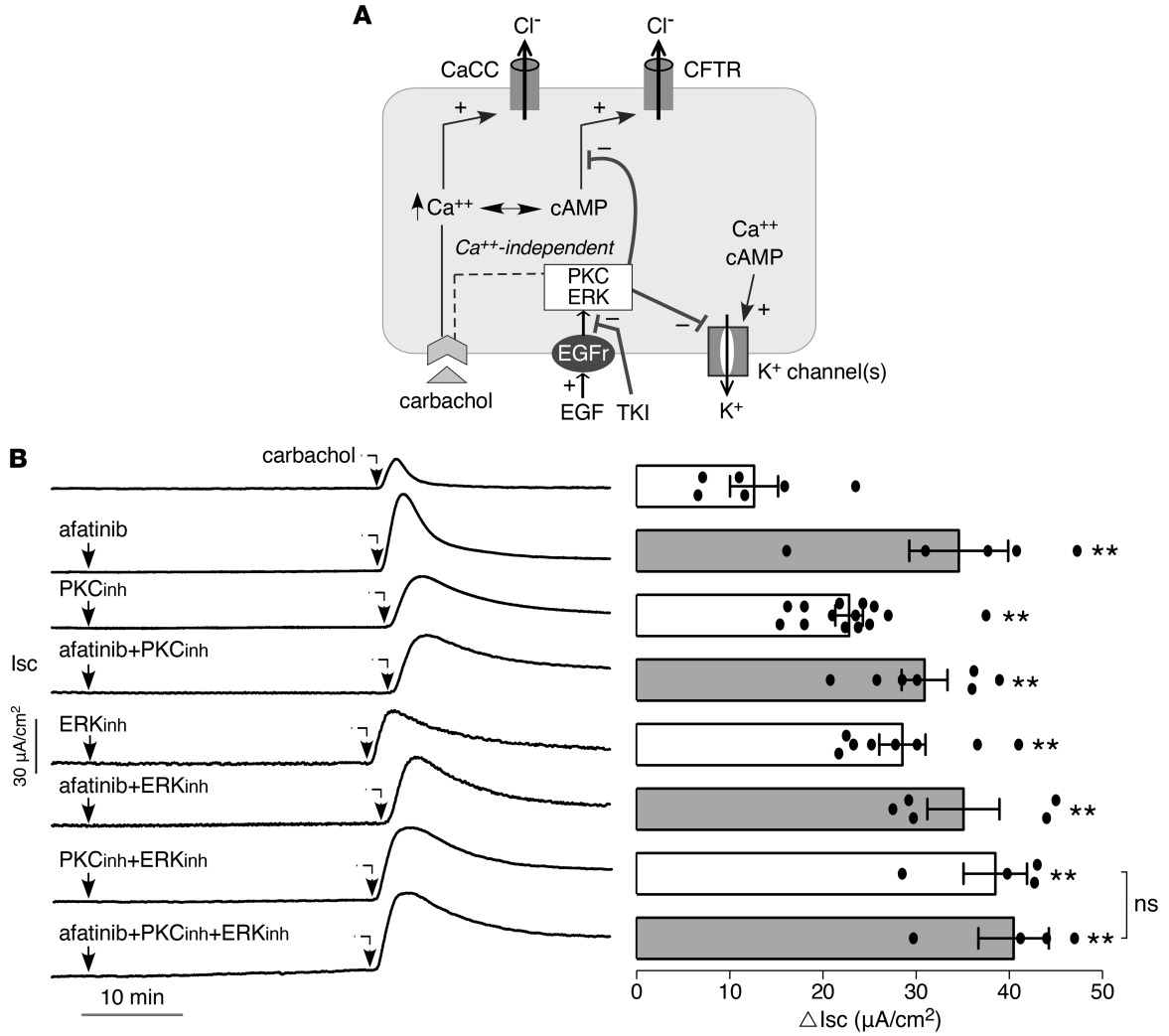

Figure 8. Involvement of ERK and PKC signaling in afatinib amplification of secretion. (**A**) Schematic of proposed mechanism of TKI action. EGF binding to its receptor (EGFR) inhibits activation of basolateral K^+ channels and apical Cl^- channels via PKC and ERK signaling. TKI abolishes this inhibition. (**B**) (Left) short-circuit current in T84 cells showing responses to afatinib (20 μM), PKC inhibitor (Ro-31-8220, 10 μM), ERK inhibitor (GDC-0994, 10 μM), alone or together, added 25 minutes before 100 μM carbachol. (Right) summary of peak carbachol-induced current (mean ± SEM, n = 4–14). $^{**}P < 0.01$, by 2-tailed t test.

Methods

Chemicals. Lapatinib and gefitinib were purchased from Synkinase and afatinib from Abcam. BAPTA-AM was purchased from EMD Millipore. Clotrimazole was purchased from Spectrum Chemicals and senicapoc from MedChem Express. PKC inhibitor Ro-31-8220 was purchased from Tocris Bioscience and ERK inhibitor GDC-0994 from APExBIO. EGF and thapsigargin were purchased from Abcam. Forskolin, carbachol, and other chemicals were purchased from Sigma-Aldrich. $CFTR_{inh}$-172 and (R)-BPO-27 (herein called BPO-27) were synthesized and purified as described previously (47, 60, 61).

Cell culture. T84 cells (ATCC CCL-248) were cultured in a 1:1 mixture of DMEM/Ham's F-12 medium supplemented with 10% FBS, 100 U/ml penicillin and 100 μg/ml streptomycin. Cells were grown on Snapwell inserts (Costar Corning) at 37°C in 5% CO_2/95% air and used 7 to 10 days after plating.

Short-circuit current measurement. T84 cells were mounted in Ussing chambers and bathed in symmetrical HCO_3^--buffered solution containing (in mM) 120 NaCl, 5 KCl, 1 $MgCl_2$, 1 $CaCl_2$, 10 D-glucose, 5 HEPES, and 25 $NaHCO_3$ (pH 7.4). The solutions were aerated with 95% O_2/5% CO_2 and maintained at 37°C. For measurement of basolateral K^+ conductance, a mucosal-to-serosal K^+ gradient was established using solutions containing K^+ as the major charge-carrying ion. The apical solution contained (in mM) 142.5 K-gluconate, 1.25 $CaCl_2$, 0.40 $MgSO_4$, 0.43 KH_2PO_4, 0.35 Na_2HPO_4, 10 HEPES, and 5.6 D-glucose, pH 7.4. In basolateral solution 142.5 mM K-gluconate was replaced by 5.4 mM K-gluconate and 136.9 mM *N*-methylglucamine,

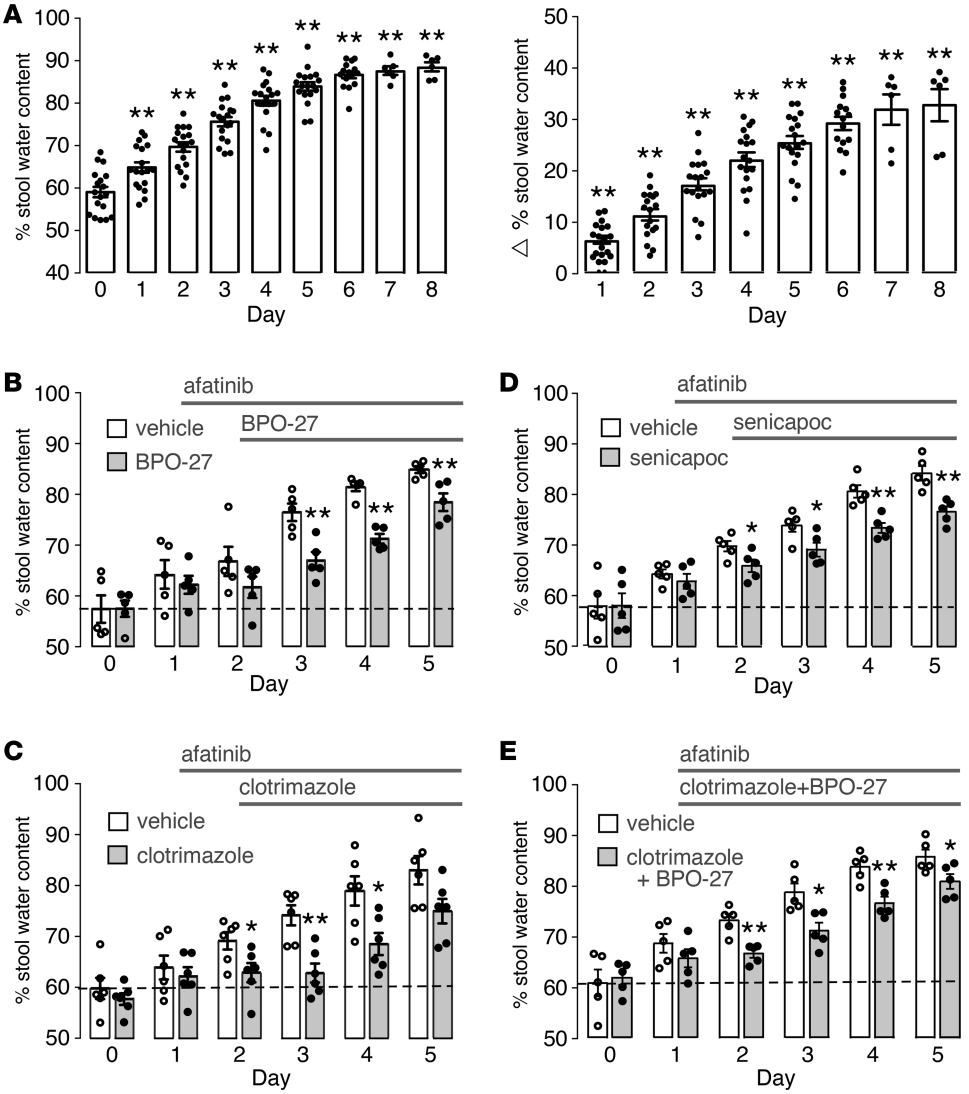

Figure 9. Inhibitors of K^+ channels and CFTR Cl^- channels reduce afatinib-induced diarrhea in rats. (**A**) Afatinib diarrhea model in Sprague-Dawley rats administered afatinib orally (60 mg/kg, daily). (Left) stool water content (percentage water) as measured daily. (Right) increase in stool water content in individual rats (stool water at indicated data minus stool water on day 0 in same rats). (**B**) Rats were administered afatinib starting on day 1 and treated starting on day 2 with BPO-27 (10 mg/kg, twice daily, intraperitoneally) or vehicle (mean ± SEM, n = 5 rats per group). (**C**) Similar protocol as in (**B**), except for treatment with clotrimazole (100 mg/kg, oral, in 2 divided doses) or vehicle (mean ± SEM, n = 6 rats per group). (**D**) Similar protocol as in (**B**), except for treatment with senicapoc (30 mg/kg, oral, twice daily) or vehicle (mean ± SEM, n = 5 rats per group). (**E**) Similar protocol except for treatment starting on day 1 with clotrimazole and BPO-27, same doses as in (**B**) and (**C**), or vehicle (mean ± SEM, n = 5 rats per group). *P < 0.05, **P < 0.01, comparing with day 0 in (**A**) and with versus without drug treatment in **B**–**E**.

and the apical membrane was permeabilized with 20 μM amphotericin B (32). For measurement of apical Cl^- conductance, a basolateral-to-apical Cl^- gradient was applied. The basolateral solution contained (in mM) 120 NaCl, 1 $MgCl_2$, 1 $CaCl_2$, 10 D-glucose, 5 HEPES, and 25 $NaHCO_3$ (pH 7.4). In the apical solution 120 mM NaCl was replaced by 5 mM NaCl and 115 mM Na-gluconate, and the basolateral membrane was permeabilized with 250 μg/ml amphotericin B (62). Short-circuit current was measured using an EVC4000 multichannel voltage clamp (World Precision Instruments). For intestinal short-circuit current measurement, CD1 mice were anesthetized with isoflurane. The ileum was removed, washed with ice-cold Krebs buffer, and opened along the mesenteric border, and a full-thickness layer was mounted in a micro-Ussing chamber (area 0.7 cm^2, World Precision Instruments). Hemichambers were filled with oxygenated Krebs-Ringer bicarbonate solution.

Intracellular calcium and cAMP measurements. T84 cells were plated in 96-well, black-walled microplates. Confluent cells were loaded with Fluo-4 NW (Invitrogen) at 72 hours after plating. In some studies cells

were pretreated for 30 minutes with afatinib. Fluo-4 fluorescence was measured with a Tecan Infinite M1000 plate reader (Tecan Group Ltd.) at excitation/emission wavelengths of 495/516 nm. For cAMP assay, T84 cells were grown in 24-well plates, treated for 30 minutes with afatinib and/or forskolin, lysed by repeating freeze/thaw, and centrifuged to remove cell debris, and the supernatant was assayed for cAMP using the cAMP Parameter immunoassay kit according to the manufacturer's instructions (R&D Systems).

Rat model of afatinib diarrhea. Female Sprague-Dawley rats (ages 8–10 weeks, purchased from Charles River) received oral afatinib (60 mg/kg oral) daily for 6 days. BPO-27 (10 mg/kg, intraperitoneally), clotrimazole (100 mg/kg, oral) or senicapoc (30 mg/kg, oral), or (R)-BPO-27 plus clotrimazole, was administered twice daily to afatinib-treated rats. (R)-BPO-27 and senicapoc were dissolved in saline containing 5% DMSO and 10% Kolliphor HS. Clotrimazole was dispersed in peanut oil and sonicated for 30 minutes. Rats were placed individually in metabolic cages and given access to water and food. Stool samples were collected for 5 hours. To measure stool water content, the stool samples were dried at 70°C for 24 hours, and water content was calculated as (wet weight – dry weight) / wet weight.

Statistics. Data are presented as mean ± SEM. Statistical analysis was performed using Prism 5 GraphPad software package. Statistical comparisons were made using Student's *t* test or ANOVA. A value of $P < 0.05$ was taken as statistically significant.

Study approval. Animal experiments were approved by the UCSF IACUC.

Author contributions

TD performed in vitro and in vivo experiments. TD, OC, and ASV designed experiments and analyzed data. TD, OC, JRT, and ASV wrote and edited the manuscript. JRT and ASV conceived the original idea for this study.

Acknowledgments

This work was supported by grants DK099803, DK72517, DK101373, EY13574, and EB00415 from the NIH; grants from the Cystic Fibrosis Foundation; and a sponsored research agreement from Vanda Pharmaceutics (Washington, DC). We thank Mark Donowitz (Johns Hopkins) and Jerry Turner (Harvard) for helpful suggestions.

Address correspondence to: Alan S. Verkman, 1246 Health Sciences East Tower, 513 Parnassus Ave., University of California, San Francisco, California 94143-0521, USA. Phone: 415.476.8530; Email: Alan.Verkman@ucsf.edu.

1. Stein A, Voigt W, Jordan K. Chemotherapy-induced diarrhea: pathophysiology, frequency and guideline-based management. *Ther Adv Med Oncol*. 2010;2(1):51–63.
2. Oun R, Moussa YE, Wheate NJ. The side effects of platinum-based chemotherapy drugs: a review for chemists. *Dalton Trans*. 2018;47(19):6645–6653.
3. Grabenbauer GG, Holger G. Management of radiation and chemotherapy related acute toxicity in gastrointestinal cancer. *Best Pract Res Clin Gastroenterol*. 2016;30(4):655–664.
4. Touchefeu Y, et al. Systematic review: the role of the gut microbiota in chemotherapy- or radiation-induced gastrointestinal mucositis — current evidence and potential clinical applications. *Aliment Pharmacol Ther*. 2014;40(5):409–421.
5. McQuade RM, Stojanovska V, Abalo R, Bornstein JC, Nurgali K. Chemotherapy-induced constipation and diarrhea: pathophysiology, current and emerging treatments. *Front Pharmacol*. 2016;7:414.
6. Kornblau S, et al. Management of cancer treatment-related diarrhea. Issues and therapeutic strategies. *J Pain Symptom Manage*. 2000;19(2):118–129.
7. Van Sebille YZ, Gibson RJ, Wardill HR, Bowen JM. ErbB small molecule tyrosine kinase inhibitor (TKI) induced diarrhoea: Chloride secretion as a mechanistic hypothesis. *Cancer Treat Rev*. 2015;41(7):646–652.
8. Bowen JM, et al. Development of a rat model of oral small molecule receptor tyrosine kinase inhibitor-induced diarrhea. *Cancer Biol Ther*. 2012;13(13):1269–1275.
9. Pessi MA, et al. Targeted therapy-induced diarrhea: A review of the literature. *Crit Rev Oncol Hematol*. 2014;90(2):165–179.
10. Hirsh V, Blais N, Burkes R, Verma S, Croitoru K. Management of diarrhea induced by epidermal growth factor receptor tyrosine kinase inhibitors. *Curr Oncol*. 2014;21(6):329–336.
11. Shepherd FA, et al. Erlotinib in previously treated non-small-cell lung cancer. *N Engl J Med*. 2005;353(2):123–132.
12. Yang JC, et al. Diarrhea associated with afatinib: an oral ErbB family blocker. *Expert Rev Anticancer Ther*. 2013;13(6):729–736.
13. Aw DC, Tan EH, Chin TM, Lim HL, Lee HY, Soo RA. Management of epidermal growth factor receptor tyrosine kinase inhibitor-related cutaneous and gastrointestinal toxicities. *Asia Pac J Clin Oncol*. 2018;14(1):23–31.
14. Thiagarajah JR, Donowitz M, Verkman AS. Secretory diarrhoea: mechanisms and emerging therapies. *Nat Rev Gastroenterol Hepatol*. 2015;12(8):446–457.

15. Frizzell RA, Hanrahan JW. Physiology of epithelial chloride and fluid secretion. *Cold Spring Harb Perspect Med*. 2012;2(6):a009563.
16. Barrett KE, Keely SJ. Chloride secretion by the intestinal epithelium: molecular basis and regulatory aspects. *Annu Rev Physiol*. 2000;62:535–572.
17. Matos JE, Sausbier M, Beranek G, Sausbier U, Ruth P, Leipziger J. Role of cholinergic-activated KCa1.1 (BK), KCa3.1 (SK4) and KV7.1 (KCNQ1) channels in mouse colonic Cl- secretion. *Acta Physiol (Oxf)*. 2007;189(3):251–258.
18. Cil O, et al. Benzopyrimido-pyrrolo-oxazine-dione CFTR inhibitor (R)-BPO-27 for antisecretory therapy of diarrheas caused by bacterial enterotoxins. *FASEB J*. 2017;31(2):751–760.
19. Ko EA, Jin BJ, Namkung W, Ma T, Thiagarajah JR, Verkman AS. Chloride channel inhibition by a red wine extract and a synthetic small molecule prevents rotaviral secretory diarrhoea in neonatal mice. *Gut*. 2014;63(7):1120–1129.
20. Thiagarajah JR, Broadbent T, Hsieh E, Verkman AS. Prevention of toxin-induced intestinal ion and fluid secretion by a small-molecule CFTR inhibitor. *Gastroenterology*. 2004;126(2):511–519.
21. Uribe JM, Gelbmann CM, Traynor-Kaplan AE, Barrett KE. Epidermal growth factor inhibits Ca(2+)-dependent Cl^- transport in T84 human colonic epithelial cells. *Am J Physiol*. 1996;271(3 pt 1):C914–C922.
22. Keely SJ, Barrett KE. ErbB2 and ErbB3 receptors mediate inhibition of calcium-dependent chloride secretion in colonic epithelial cells. *J Biol Chem*. 1999;274(47):33449–33454.
23. Cuthbert AW, Hickman ME, Thorn P, MacVinish LJ. Activation of Ca(2+)- and cAMP-sensitive K(+) channels in murine colonic epithelia by 1-ethyl-2-benzimidazolone. *Am J Physiol*. 1999;277(1):C111–C120.
24. Singh S, Syme CA, Singh AK, Devor DC, Bridges RJ. Benzimidazolone activators of chloride secretion: potential therapeutics for cystic fibrosis and chronic obstructive pulmonary disease. *J Pharmacol Exp Ther*. 2001;296(2):600–611.
25. Rufo PA, Jiang L, Moe SJ, Brugnara C, Alper SL, Lencer WI. The antifungal antibiotic, clotrimazole, inhibits Cl^- secretion by polarized monolayers of human colonic epithelial cells. *J Clin Invest*. 1996;98(9):2066–2075.
26. Ataga KI, et al. Efficacy and safety of the Gardos channel blocker, senicapoc (ICA-17043), in patients with sickle cell anemia. *Blood*. 2008;111(8):3991–3997.
27. Rittenhouse AR, Vandorpe DH, Brugnara C, Alper SL. The antifungal imidazole clotrimazole and its major in vivo metabolite are potent blockers of the calcium-activated potassium channel in murine erythroleukemia cells. *J Membr Biol*. 1997;157(2):177–191.
28. McCole DF, Barrett KE. Decoding epithelial signals: critical role for the epidermal growth factor receptor in controlling intestinal transport function. *Acta Physiol (Oxf)*. 2009;195(1):149–159.
29. Sun H, Niisato N, Inui T, Marunaka Y. Insulin is involved in transcriptional regulation of NKCC and the CFTR Cl(-) channel through PI3K activation and ERK inactivation in renal epithelial cells. *J Physiol Sci*. 2014;64(6):433–443.
30. Takei S, Iseda T, Yokoyama M. Inhibitory effect of clotrimazole on angiogenesis associated with bladder epithelium proliferation in rats. *Int J Urol*. 2003;10(2):78–85.
31. Khalid MH, Tokunaga Y, Caputy AJ, Walters E. Inhibition of tumor growth and prolonged survival of rats with intracranial gliomas following administration of clotrimazole. *J Neurosurg*. 2005;103(1):79–86.
32. Rufo PA, et al. The antifungal antibiotic, clotrimazole, inhibits chloride secretion by human intestinal T84 cells via blockade of distinct basolateral K+ conductances. Demonstration of efficacy in intact rabbit colon and in an in vivo mouse model of cholera. *J Clin Invest*. 1997;100(12):3111–3120.
33. Staal RGW, et al. Inhibition of the potassium channel KCa3.1 by senicapoc reverses tactile allodynia in rats with peripheral nerve injury. *Eur J Pharmacol*. 2017;795:1–7.
34. Paka L, et al. Anti-steatotic and anti-fibrotic effects of the KCa3.1 channel inhibitor, Senicapoc, in non-alcoholic liver disease. *World J Gastroenterol*. 2017;23(23):4181–4190.
35. Chao AC, de Sauvage FJ, Dong YJ, Wagner JA, Goeddel DV, Gardner P. Activation of intestinal CFTR Cl- channel by heat-stable enterotoxin and guanylin via cAMP-dependent protein kinase. *EMBO J*. 1994;13(5):1065–1072.
36. Sears CL, Kaper JB. Enteric bacterial toxins: mechanisms of action and linkage to intestinal secretion. *Microbiol Rev*. 1996;60(1):167–215.
37. Subramanya SB, Rajendran VM, Srinivasan P, Nanda Kumar NS, Ramakrishna BS, Binder HJ. Differential regulation of cholera toxin-inhibited Na-H exchange isoforms by butyrate in rat ileum. *Am J Physiol Gastrointest Liver Physiol*. 2007;293(4):G857–G863.
38. Hecht G, et al. Differential regulation of Na^+/H^+ exchange isoform activities by enteropathogenic E. coli in human intestinal epithelial cells. *Am J Physiol Gastrointest Liver Physiol*. 2004;287(2):G370–G378.
39. Lundgren O, Peregrin AT, Persson K, Kordasti S, Uhnoo I, Svensson L. Role of the enteric nervous system in the fluid and electrolyte secretion of rotavirus diarrhea. *Science*. 2000;287(5452):491–495.
40. Stocker JW, De Franceschi L, McNaughton-Smith GA, Corrocher R, Beuzard Y, Brugnara C. ICA-17043, a novel Gardos channel blocker, prevents sickled red blood cell dehydration in vitro and in vivo in SAD mice. *Blood*. 2003;101(6):2412–2418.
41. Crowley PD, Gallagher HC. Clotrimazole as a pharmaceutical: past, present and future. *J Appl Microbiol*. 2014;117(3):611–617.
42. Brugnara C, et al. Therapy with oral clotrimazole induces inhibition of the Gardos channel and reduction of erythrocyte dehydration in patients with sickle cell disease. *J Clin Invest*. 1996;97(5):1227–1234.
43. Rifai N, et al. HPLC measurement, blood distribution, and pharmacokinetics of oral clotrimazole, potentially useful antisickling agent. *Clin Chem*. 1995;41(3):387–391.
44. Suzuki S, Kurata N, Nishimura Y, Yasuhara H, Satoh T. Effects of imidazole antimycotics on the liver microsomal cytochrome P450 isoforms in rats: comparison of in vitro and ex vivo studies. *Eur J Drug Metab Pharmacokinet*. 2000;25(2):121–126.
45. Ataga KI, et al. Dose-escalation study of ICA-17043 in patients with sickle cell disease. *Pharmacotherapy*. 2006;26(11):1557–1564.
46. Ataga KI, Stocker J. Senicapoc (ICA-17043): a potential therapy for the prevention and treatment of hemolysis-associated complications in sickle cell anemia. *Expert Opin Investig Drugs*. 2009;18(2):231–239.
47. Snyder DS, Tradtrantip L, Yao C, Kurth MJ, Verkman AS. Potent, metabolically stable benzopyrimido-pyrrolo-oxazine-dione (BPO) CFTR inhibitors for polycystic kidney disease. *J Med Chem*. 2011;54(15):5468–5477.
48. Van Sebille YZA, Gibson RJ, Wardill HR, Ball IA, Keefe DMK, Bowen JM. Dacomitinib-induced diarrhea: Targeting chloride secretion with crofelemer. *Int J Cancer*. 2018;142(2):369–380.
49. Tradtrantip L, Namkung W, Verkman AS. Crofelemer, an antisecretory antidiarrheal proanthocyanidin oligomer extracted from

Croton lechleri, targets two distinct intestinal chloride channels. *Mol Pharmacol*. 2010;77(1):69–78.
50. Heitzmann D, Warth R. Physiology and pathophysiology of potassium channels in gastrointestinal epithelia. *Physiol Rev*. 2008;88(3):1119–1182.
51. Halm DR. Secretory control of basolateral membrane potassium and chloride channels in colonic crypt cells. *Adv Exp Med Biol*. 2004;559:119–129.
52. Iliev IG, Marino AA. Potassium channels in epithelial cells. *Cell Mol Biol Res*. 1993;39(6):601–611.
53. Chow JY, Uribe JM, Barrett KE. A role for protein kinase cepsilon in the inhibitory effect of epidermal growth factor on calcium-stimulated chloride secretion in human colonic epithelial cells. *J Biol Chem*. 2000;275(28):21169–21176.
54. Keely SJ, Uribe JM, Barrett KE. Carbachol stimulates transactivation of epidermal growth factor receptor and mitogen-activated protein kinase in T84 cells. Implications for carbachol-stimulated chloride secretion. *J Biol Chem*. 1998;273(42):27111–27117.
55. Bertelsen LS, Barrett KE, Keely SJ. Gs protein-coupled receptor agonists induce transactivation of the epidermal growth factor receptor in T84 cells: implications for epithelial secretory responses. *J Biol Chem*. 2004;279(8):6271–6279.
56. McCole DF, Keely SJ, Coffey RJ, Barrett KE. Transactivation of the epidermal growth factor receptor in colonic epithelial cells by carbachol requires extracellular release of transforming growth factor-alpha. *J Biol Chem*. 2002;277(45):42603–42612.
57. Lin AL, et al. Distinct pathways of ERK activation by the muscarinic agonists pilocarpine and carbachol in a human salivary cell line. *Am J Physiol, Cell Physiol*. 2008;294(6):C1454–C1464.
58. Clark JA, et al. Involvement of the ERK signaling cascade in protein kinase C-mediated cell cycle arrest in intestinal epithelial cells. *J Biol Chem*. 2004;279(10):9233–9247.
59. Graness A, Chwieralski CE, Reinhold D, Thim L, Hoffmann W. Protein kinase C and ERK activation are required for TFF-peptide-stimulated bronchial epithelial cell migration and tumor necrosis factor-alpha-induced interleukin-6 (IL-6) and IL-8 secretion. *J Biol Chem*. 2002;277(21):18440–18446.
60. Snyder DS, et al. Absolute configuration and biological properties of enantiomers of cftr inhibitor BPO-27. *ACS Med Chem Lett*. 2013;4(5):456–459.
61. Ma T, et al. Thiazolidinone CFTR inhibitor identified by high-throughput screening blocks cholera toxin-induced intestinal fluid secretion. *J Clin Invest*. 2002;110(11):1651–1658.
62. Pongkorpsakol P, Pathomthongtaweechai N, Srimanote P, Soodvilai S, Chatsudthipong V, Muanprasat C. Inhibition of cAMP-activated intestinal chloride secretion by diclofenac: cellular mechanism and potential application in cholera. *PLoS Negl Trop Dis*. 2014;8(9):e3119.